Stereological Evaluation of Rabbit Fetus Liver after Xenotransplantation of Human Wharton's Jelly-Derived Mesenchymal Stromal Cells

Z. Khodabandeh[1], L. Rezaeian[2], M. A. Edalatmanesh[3], A. Mogheiseh[4], N. Tanideh[1,5], M. Dianatpour[1,6], Sh. Zare[1], H. Bordbar[7,8], N. Baghban[8], A. Tamadon[9]*

[1]*Stem Cells Technology Research Center, Shiraz University of Medical Sciences, Shiraz, Iran*
[2]*Department of Biology, Faculty of Sciences, Farhangian University, Tehran, Iran*
[3]*Department of Biology, Faculty of Sciences, Shiraz Branch, Islamic Azad University, Shiraz, Iran*
[4]*Department of Clinical Sciences, School of Veterinary Medicine, Shiraz University, Shiraz, Iran*
[5]*Department of Pharmacology, School of Medicine, Shiraz University of Medical Sciences, Shiraz, Iran*
[6]*Department of Human Genetics, School of Medicine, Shiraz University of Medical Sciences, Shiraz, Iran*
[7]*Histomorphometry and Stereology Research Center, Shiraz University of Medical Science, Shiraz, Iran*
[8]*Department of Anatomy, Shiraz University of Medical Sciences, Shiraz, Iran*
[9]*PerciaVista R&D Co. Shiraz, Iran*

ABSTRACT

Background: In-utero xenotransplantation of stem cells in abnormal fetuses effectively treats several genetic illnesses.

Objective: The current research aimed to evaluate structural and morphological alterations in the liver of rabbit fetuses following xenotransplantation of human Wharton's jelly-derived mesenchymal stromal cells (hWJ-MSCs), using a stereological technique.

Methods: All hWJ-MSCs were isolated from the human umbilical cord, and their authenticity was established by flow-cytometry and differentiation. At gestational day 14, the rabbits were anesthetized, and hWJ-MSCs were injected into the uteri of 24 fetuses. Twenty-two fetuses were born successfully. Ten rabbit liver specimens were prepared from injected fetuses including; eight rabbits on day three following birth and two rabbits on the 21st post-natal day. The non-injected fetuses were considered positive controls. The livers of the control and hWJ-MSCs-treated rabbits were fixed, processed, stained, and examined through stereological approaches.

Results: In the hWJ-MSCs-treated group, the mean liver weight and volume increased by 42% and 78% compared to the control group. The total volume of the hepatocytes increased by 63%, and that of sinusoids by three folds in the treated rabbits. The total volume of the central veins increased by 70%. The total number corresponding to hepatocytes in the experimental group increased by 112% compared to the rabbits in the control. The total volume of the hepatocyte nuclei in the experimental group increased by 117% compared to the rabbits in the control.

Conclusion: After xenotransplantation of human MSCs, host tissue microenvironments (here, the rabbit liver) were altered and these included quantitative factors corresponding to the liver tissue and hepatocyte morphometric indices.

KEYWORDS: Xenotransplantation; Mesenchymal stromal/stem cells; Wharton's jelly; Stereology; Liver

INTRODUCTION

Liver function is crucial in maintaining body homeostasis, while their disorders cause significant morbidity and mortality [1]. Liver transplantation has long been considered as the only curative option for acute or chronic liver disorders in its progressive phases [2]. While liver transplantation is generally involved with critical concerns; regenerative treatments have been known as minimally invasive procedures with few adverse effects [3, 4].

In this context, stem cells with diverse origins have been studied for curing hepatic diseas-

*Correspondence: Amin Tamadon, DVM, PhD
PerciaVista R&D Co. Shiraz, Iran; Postal Code: 7514633196
ORCID: 0000-0002-0222-3035
Tel/Fax: +98-77-3332-8724
E-mail: amintamaddon@yahoo.com

es [5, 6]. Stem cells can be easily harvested, proliferated, and bare vast differentiation capacities [7, 8]. Wharton's jelly mesenchymal stromal/stem cells (WJ-MSCs), which are derived from the umbilical cord matrix, have been considered as one of the best sources for stem cell harvesting, by virtue of their non-invasive collection, immediate obtainability with a prolific donor pool, remarkable in vitro expandable values, and multi-potent differentiation [9, 10]. WJ-MSCs have potentials for cell therapy [11] and hold a remarkably higher proliferation rate and expression level of early endodermal, undifferentiated human embryonic and pluripotent stem cell markers, both at primary and late passages [12].

The extensive scarcity of human tissues, organs, and cells suitable for transplantation, is the underlying reason for the current rise in xenotransplantation popularity, allowing transplantation between various species. Non-human mammals, the most immediate human relatives, were initially counted on as potential organ xenotransplantation sources [13]. The rabbit has assumed the most appropriate species for this purpose because of its physiological suitability, breeding properties, and anatomical resemblance [14].

Furthermore, a treatment approach called xenotransplantation of the hWJ-MSCs was introduced that helps the human liver reconstruction in the rabbit's embryo [15]. While, much literature exists on evaluating physiological and biochemical liver function after xenotransplantation [16, 17]; There are few studies done on post-xenotransplantation changes in liver histological structure. Studies on the evaluation of liver regeneration and surgical techniques require quantification [18]. Furthermore, the durability of transplanted cell populations should be evaluated by an unbiased method such as stereology [19]. The current investigation examines the impact of hWJ-MSCs xenotransplantation on liver volume, total volume of hepatocytes, sinusoids, and central veins among rabbit fetuses.

MATERIALS AND METHODS

Animals

Ten pregnant female rabbits (New Zealand white strain) weighing 2.2-3.3 kg were bought from the Center of Comparative and Experimental Medicine, Shiraz University of Medical Sciences. Ultrasonography was used to confirm their pregnancy (Hitachi EUB, Hitachi Medical Corp, Tokyo, Japan) [20]. A rabbit was chosen as a xenotransplant recipient of human cells for its capability for producing numerous infants in each pregnancy, short period of pregnancy, and simple intrauterine injection (IUI) of large fetus which increases the success rates of in-utero xenotransplantation.

Harvesting and Preparation of hWJ-MSCs

A written informed consent was attained from parents for harvesting of the umbilical cords [21]. Umbilical cord specimens were provided from 10 cesarean section deliveries of full-term infants at Hafez Hospitals, Shiraz, Iran and were immediately transported to the laboratory in cold phosphate-buffered saline (PBS) containing 100 U/mL penicillin and 100 µg/mL streptomycin (Sigma Aldrich, UK). Then, the umbilical vein was cut off to small pieces using a sterile blade, and both arteries were detached. Afterward, the tissues were divided into small explant parts (approximately 4×5 mm) and moved to a culture flask. Following 15 min, α-minimum essential medium (α-MEM, Sigma, USA) containing 10% fetal bovine serum (FBS, Gibco BRL), 1% L-glutamine (Sigma Aldrich, UK), 100 U/mL penicillin, and 100 µg/mL streptomycin was poured into the culture flask, and the old medium was changed 2-times a week over the experimentation period. The MSCs reached 70-80% confluence after two weeks.

Flow-cytometry Assessment of hWJ-MSCs

Flow cytometry was used for detecting the specific marker of the MSCs and their multiplicity in hWJ-MSCs. The cells at the third passage were separated and resuspended in cold 10% FBS/PBS as an obstructive solution for 20 min. After that, MSCs were incubated with fluorescein isothiocyanate (FITC) conjugated with anti-CD-144 and CD-44, Perce-

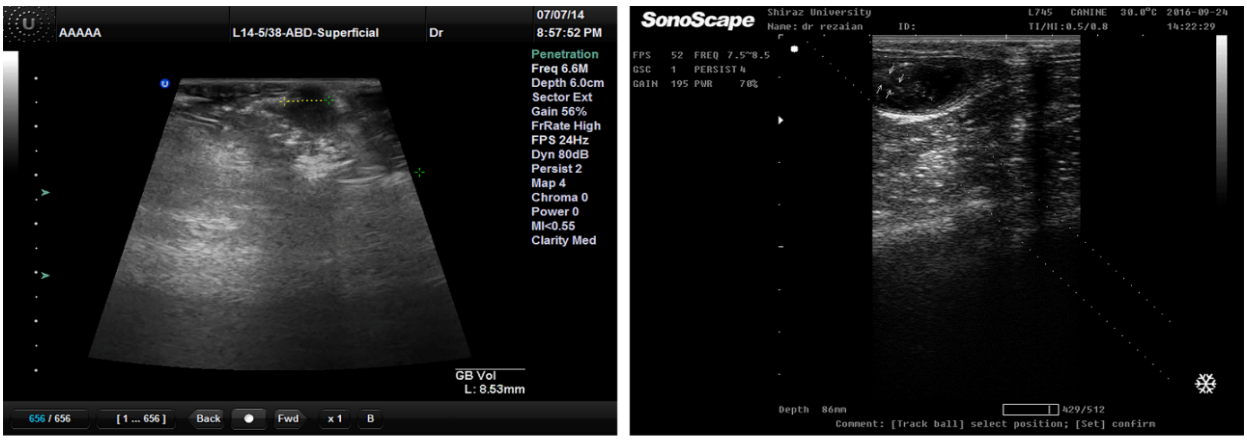

Figure 1: Intrauterine injection of human Wharton's jelly-derived mesenchymal stromal/stem cells (hWJ-MSCs) into the fetuses of the studied animal after determining the exact place corresponding to the peritoneal cavity using ultrasonography. **A**) measuring crown-rump length corresponding to the fetuses. **B**) inserting a needle (arrows) and injecting hWJ-MSCs in the fetus peritoneal cavity (arrows).

conjugated anti-CD-105, and phycoerythrin-conjugated anti-CD-34 and CD106 (all from Abcam, Cambridge, UK) for 30 min. Next, the cells were eluted two times and suspended in cold PBS. The percentage of positive or negative cells was assessed using a calibrated Fluorescence-activated cell sorting (FACS) device and analyzed by FlowJo software.

Differentiation of hWJ-MSCs into Osteogenic and Adipogenic Lineages

To differentiate hWJ-MSCs to osteogenic and adipogenic lineage [15], 1×10^4 cells at the fourth passage were cultured in 24 wells plates. After reaching the cells confluence to around 80%, the previous medium was replaced with osteogenic medium (comprising of DMEM-LG with 10% FBS, 2 mM L-glutamine, 100 U/mL penicillin, 100 µg/mL streptomycin, 100 nM dexamethasone, 0.2 mM L-ascorbate and 10 mM β-glycerophosphate) or adipogenic medium (comprising of DMEM-LG with 10% FBS, 2 mM of L-glutamine, 100 U/mL penicillin, 100 µg/mL streptomycin, 60 µM indomethacin, 1 µM dexamethasone, 0.5 mM of IBMX and 5 µg/mL Insulin solution). The cells in osteogenic and adipogenic media were incubated for 28 and 21 days, respectively. Half of each medium was changed every three days. For differentiation assessment, both differentiated cell lines were fixed in 4% paraformaldehyde and then stained with Alizarin and oil red for confirming differentiated bone cells and lipid cells, respectively.

In-utero Xenotransplantation

Rabbits produce their initial antibody stock by VDJ gene rearrangement in the fetal liver as early as gestation day 14 [22]. Considering the onset of development in rabbits' immune systems, in utero xenotransplantation was carried out on day 14 of pregnancy [23]. Eight rabbits were chosen for injecting cells. The fetuses of non-injected rabbits were categorized as positive controls, and fetuses of 2 pregnant rabbits not injected served as the negative control. Rabbits were anesthetized with an intramuscular injection of 1 mg/kg xylazine and 2 mg/kg ketamine (Alfasan, Worden, Holland) and placed in a dorsal position. A transabdominal ultrasound equipped with a 3.5-MHz curved array probe was used to determine the existence, location, and feasibility of the fetuses. Also, the fetal crown-rump length was obtained for confirming the gestational age (Fig 1A) [24].

A 24-gauge spinal needle was used to expose the uterus from an abdominal wall incision in such a way that the needle was continuously inserted into the amniotic cavity through the uterine wall, the peritoneal cavity, and liver corresponding to the fetuses under continu

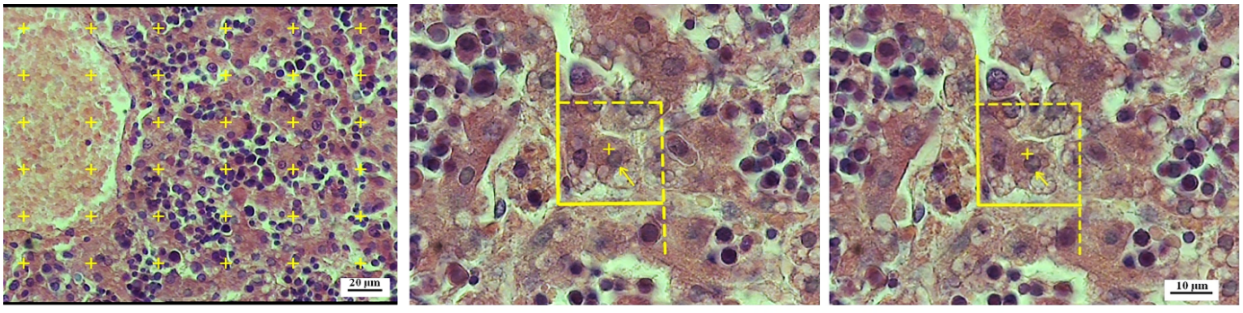

Figure 2: **A**) A microscopic section corresponding to the liver, representing the hepatocytes, sinusoids, and central vein. To approximate the volume density corresponding to histological factors of the liver, the number of total points striking each component was divided by the number of points striking the reference space. **B**) A microscopic section corresponding to the liver representing the hepatocytes. A non-biased counting frame was superimposed on the images of the 25 µm thick sections to approximate the number of total hepatocyte nuclei. A microcator was used to ignore each cell whose nucleus was in focus at the beginning 4 µm plane. **C**) Nuclei that came into full focus within the subsequent traveling 4 µm optical section were chosen if they lay in the counting frame or did not touch the exclusion boundaries of the frame and touched the inclusion boundaries of the frame.

ous ultrasound guidance with the freehand method [25, 26]. After confirming the suitable placement of the needle, the hWJ-MSCs were gradually injected in a total volume of 3×10^6/200 µL. Ultrasound images shown in Fig 1B showed the distribution of a small echogenic fluid in the peritoneal cavity over infusion. The exact process was repeated in other fetuses. The abdominal wall was sutured. The heartbeat of the fetal was controlled using ultrasonography until the dam recovery. Checking of the dams in terms of abortion symptoms and health status was performed every day. The rabbits whose fetuses were normally delivered 13 to 15 days following transplantation were entered in the next research phase. The treated animals and their controls were euthanized and quickly dissected, and their livers were removed.

Approximation of the Reference Volume and Shrinkage

Following a thorough wash and weighing of the liver, the primary volume was quantified by the immersion technique [27]. In brief, a container containing distilled water was weighed. Next, the liver was completely immersed in water using a thread to prevent it from touching the container's bottom. To calculate the liver volume in cm^3, the new weight of the container containing water was subtracted from the weight of the container containing water and liver, and the result was divided by the water-specific gravity (~1.0 kg/m3). Fixation of the liver was performed using neutral buffered formaldehyde, and it was used after one week. The deformation and shrinkage resulting from fixation, affect tissue processing and staining and a stereological approximation. Therefore, the shrinkage was approximated to guarantee absolute precision.

Approximation of some of the subsequent stereological factors needs isotropic uniform random sections [28-30], which were attained by the orientation technique. In brief, each lobe of the liver was located on a circle separated into ten equal spaces. A number between 0 and 10 was randomly chosen, and the liver lobe was split into two parts using a blade in that direction. The surface of each part was cut again after locating in the 0–0 direction of another circle with ten non-equal sinus-weighted divisions. Each lobe was divided into slabs using a blade located in the direction of the second cut with a distance of ~2 mm. Next, after a random collection of 9–11 slabs, a circle was cut from a liver slab using a trocar. The diameters corresponding to the circular section of the liver were obtained and reported in µm, and the circle area was calculated approximately using $A= \pi r^2$, in which A is the area, π is 3.1416, and r represents radius. The cut surfaces corresponding to the slabs and circular pieces were inserted in paraffin, segmented

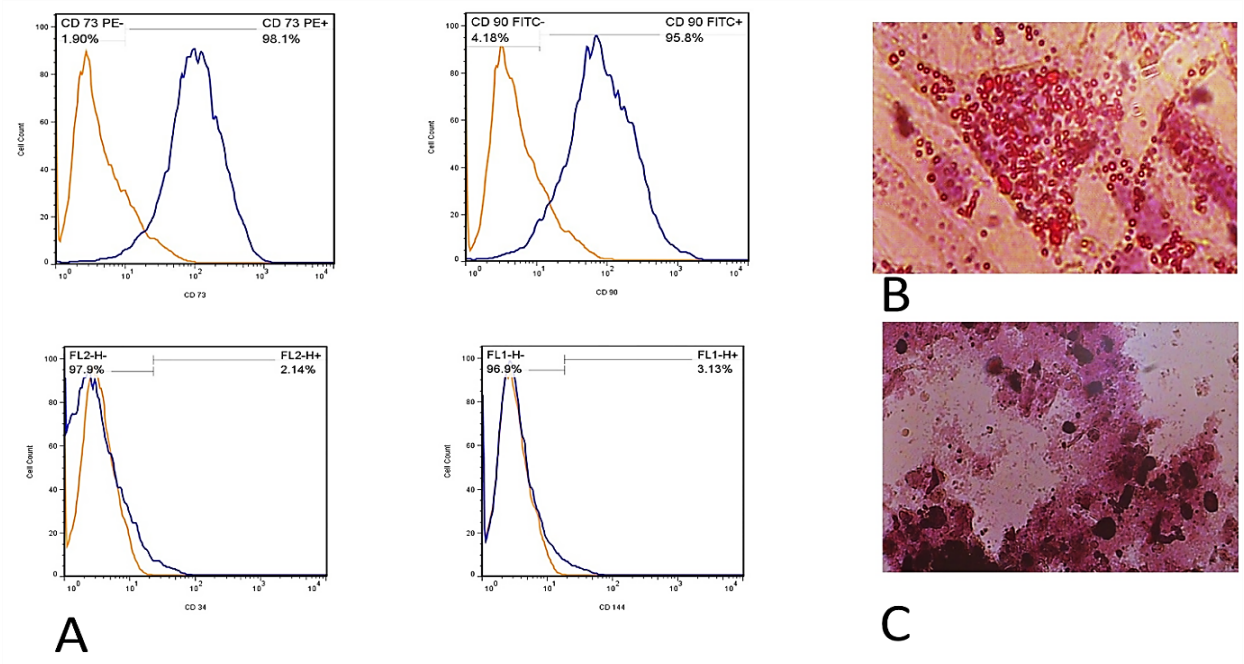

Figure 3: Confirmation of mesenchymal stromal/stem cells (MSCs) from Wharton's jelly. **A**) Phenotype by flow cytometry analysis: Expression of hWJ-MSCs surface markers (CD73 and CD90) in contrast to negative expression hematopoietic markers (CD34, CD144), **B**) Adipogenic differentiation, **C**) Osteogenic differentiation.

(4- and 25-mm thicknesses), and stained with hematoxylin and eosin. While staining was complete, the areas of the circular piece were computed again, and the volume shrinkage [28] was determined using the formula:

Volume shrinkage= 1-(AA/AB)1.5,

where 'AA' and' AB' represent the area of the circular piece post- and pre-processing, sectioning and staining, respectively. Following the shrinkage estimation, the liver's final volume (the reference space) was adjusted, using:

VFinal= VPrimary × (1- volume shrinkage).

Analysis of each sampled section was performed using a video-microscopy system which consisted of a microscope (E-200, Nikon, Japan) connected to a video camera (Sony, Japan, SSC Dc 18P), a P4 PC, and a flat monitor for the determination of the factors at a final magnification of 1500. Using a stage micrometer, 10 to 14 microscopic fields were inspected in all livers at equal intervals along the X- and Y-axis, and the procedure was performed until all the sections had been examined using stereology software designed at our laboratory. The stereological probe (composed of 25 points) was overlaid upon the images of the tissue sections observed on the monitor. A fractional volume (VV) of hepatocytes, sinusoids, nuclei, and central veins was attained using a point-counting method (Fig 2A) and the following formula:

VV= P structure/Preference in which 'P structure' and 'Preference' were the figures of test points falling on the structure's profile and the reference space, respectively.

To calculate the total volume corresponding to the factors, the fractional volume was multiplied by the liver's final volume to prevent the 'reference trap' [28, 29].

Approximation of the Number of the Hepatocyte's Nuclei

To roughly identify the number of total hepatocyte nuclei and the hepatocytes volume and their nuclei, the 25 µm thickness sections were used. Applying stereological software, overlaying a non-biased counting frame was performed on the images corresponding to

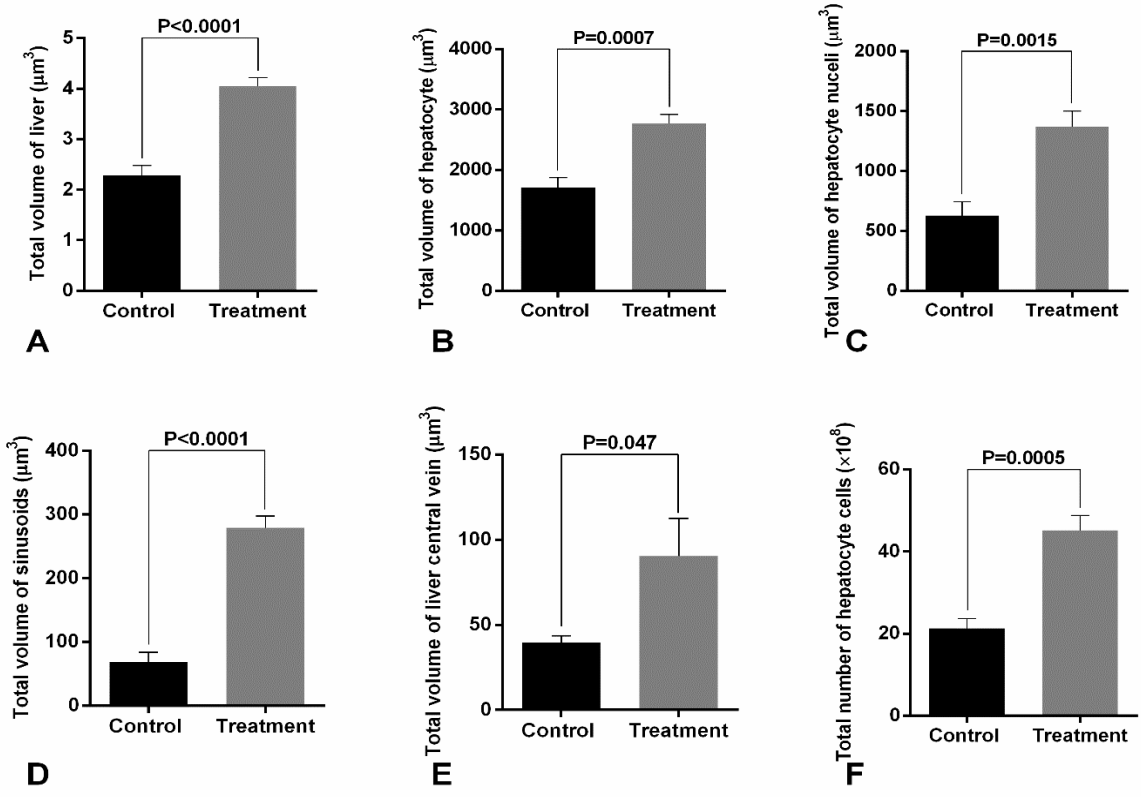

Figure 4: Comparison of stereological indices of liver tissue after xenotransplantation of human Wharton's jelly-derived mesenchymal stromal/stem cells (hWJ-MSCs) into liver corresponding to the studied animal. **A**) Total volume of liver in control and hWJ-MSCs treated rabbits, **B**) Total volume of hepatocyte in control and hWJ-MSCs treated rabbits, **C**) Total volume of hepatocyte nuclei in control and hWJ-MSCs treated rabbits, **D**) Total volume of sinusoids in control and hWJ-MSCs treated rabbits, **E**) Total volume corresponding to central veins in control and hWJ-MSCs treated rabbits, **F**) Number of total hepatocyte cells in control and hWJ-MSCs treated rabbits.

the tissue sections observed on the monitor. Averagely, 80–100 microscopic fields were chosen in each rabbit through a systematic subsample. The location of the first area was chosen randomly exterior of the sections, and the other regions were selected by changing the position of the microscope stage in equal intervals along the X- and Y-directions of the stage with a stage micrometer. A high numerical aperture 40× magnification (NA= 1.3) oil immersion lens was applied. The number of the hepatocyte nuclei was estimated using the 'dissector' technique at the final magnification of 1500.

The cells must be precisely chosen with unvarying random possibility by the 'dissector' principle to follow the technique. The optical dissector is a technique through which thick sections of cells are provided and observed using a light microscope [28, 29]. In 25 µm thickness sections, the optical section was adjusted at a random depth. An unbiased counting frame with inclusion (dotted line) and exclusion (continuous line) margins was placed over the images (Fig 2B). This frame eludes the 'edge effect' and biased counting corresponding to the particles, and a single frame was used to count all the nuclei profiles without considering their shape and have a similar possibility of being sampled. The situation of the optical section was changed toward the z-axis downwards using a microcator (Heidenhain MT-12, Germany) that measured the z-axis movements, while all cells whose nucleus was in focus at the beginning 4 mm plane were let off. Any nucleus, which came into full focus over the subsequent traveling 4 mm optical section (height of dissector), was cho-

sen only when it lay in the counting frame or touched the inclusion boundaries of the frame. The numerical density (Nv) corresponding to the cells was computed as:

$$Nv = [\Sigma Q / (\Sigma P \times (a/f) \times h)] \times (t/BA)$$

where 'ΣQ' represents the total number counted (here 175 per rabbit on the average), 'ΣP' is the number of total points falling on the hepatocyte (here 112 points per rabbit on the average), "a/f" refers to the area corresponding to the counting frame (here 576 μm2), "h" is the height of the dissector (here 12 μm), "t" represents the mean thickness section measured at diverse points of the section that was obtained as 24±0.2 μm. BA shows the setting of the microtome to cut the block (here 25 μm).

Ethical Considerations

The trials were performed based on the ethical instructions on research on laboratory animals in Shiraz University of Medical Sciences. All trials were approved by the Shiraz University of Medical Sciences ethical committee (project# IR.MIAU.REC.1396.603).

Statistical Analysis

The data were represented as mean and standard errors. Statistical differences between group means were compared by unpaired sample t-test. P values less than 0.05 were considered significant. The software of GraphPad Prism (Inc., San Diego, CA, USA) was applied for analyzing the data.

RESULTS

hWJ-MSCs Characterizations

The results of flow cytometric evaluation of hWJ-MSC at the third passage revealed the MSCs phenotype by expression of the surface markers, such as CD90 (thy-1), CD73 (ecto-5'-nucleotidase), CD44 (adhesion molecule for hyaluronic acid), CD106, and CD106 (cell adhesion molecules). However, these cells were negative for CD34 and CD144 (hematopoietic stem cell and endothelial cell markers, respectively). These proved that the isolated cells were truly MSCs (Fig 3A).

After 21 days of co-incubation in osteogenic and adipogenic media, the osteogenesis and adipogenesis of hWJ-MSCs were assessed by the Alizarin and oil Red staining methods. Image analysis proved a cumulative intensity in the area of Oil Red and Alizarin staining per cell in cells at early passages. Observing fat droplets in the cytoplasm corresponding to the hWJ-MSC confirmed adipogenic differentiation (Fig 3B). The presence of intracellular calcium displayed in Alizarin staining indicated the differentiation of cells into bone (Fig 3C).

hWJ-MSCs In-utero Xenotransplantation Increased Stereological Indices of Rabbit Livers

Twenty-seven fetuses were born healthy. Ten liver specimens were provided from injected fetuses, eight rabbits on day 3 and two rabbits on day 21 after birth. Data analysis demonstrated that the liver volume, the total volume corresponding to the hepatocytes, total volume corresponding to the hepatocyte's nuclei, the total volume of sinusoids, the total volume of central veins, and total number relating to hepatocytes cells significantly increased in hWJ-MSC treated cells comparing with the control group (Fig 4).

The mean liver volume in the hWJ-MSCs-treated group was 1.8 times more than the control group ($P<0.0001$). Furthermore, the average total volume of the hepatocytes in the hWJ-MSCs-treated group was 1.6 times more than the control group ($P=0.0007$). At the same time, the normal human liver had 4 times larger hepatocytes than the hWJ-MSCs-treated group (Table 1).

In addition, the mean total volume of the hepatocyte's nuclei in the hWJ-MSCs-treated group was 2.2 times more than the control group ($P=0.0015$). In contrast to cell volume, the nuclear volume of normal human hepatocytes was 1.7 times smaller than the hWJ-MSCs-treated group (Table 1).

The mean total volume of sinusoids in the hWJ-MSCs-treated group was 4.1 times more than the control group ($P<0.0001$). Compar

Table 1: Mean of stereological indices of liver tissue after xenotransplantation corresponding to human Wharton's jelly-derived mesenchymal stromal/stem cells (hWJ-MSCs) into rabbit fetuses' liver in the current research with human liver tissue stereological indices [33].

Stereological indices	Liver tissue of		
	Rabbit	hWJ-MSCs-treated rabbit	Human
Total volume of hepatocyte (μm^3)	1705±166.7	2769±153.9	11305±803
Total volume of hepatocyte nuclei (μm^3)	629.8±112.8	1371±132.2	798±27
Total volume of sinusoids (μm^3)	68.16±15.26	279.6±17.76	207±14

ing the extra hepatocyte space between the normal liver of human and the hWJ-MSCs-treated group did not show a noticeable difference (Table 1).

The mean total volume of central veins in the hWJ-MSCs-treated group was 2.3 times more than the control group (P=0.047). The mean total number of hepatocytes cells in the hWJ-MSCs-treated group was 2.1 times more than the control group (P=0.0005).

DISCUSSION

The modern stereological methods applied in our study for measuring hepatocytes' number represented a rise in cells numbers. Besides differences in dose and period, the key difference of our study lies in the methodological approach used for cell number evaluation. The unreliability of cell number approximation by counting structure profile in the unit area has been proved. Accordingly, it is suggested that all numerical approximations be carried out using the dissector technique [36], multiplying density by volume.

The mean volume corresponding to hepatocyte stereological indices increased after xenotransplantation. The numerical density and the volume fractions corresponding to hepatocytes in the liver have been evaluated by stereological approaches for mice [31], rats [32], and humans [33]. The effects of recipient tissue's microenvironment on behavior and morphology of transplanted human cells have been shown in mice brains [34]. It has been suggested that fusion between a recipient and transplanted cells is a phenomenon that may be affected by the microenvironment [34]. This phenomenon may impact apparent transplanted cell marker expression and cellular behavior [34].

Assuming that the enhanced total volume corresponding to the hepatocytes could be because of either hyperplasia or hypertrophy of the liver cells, the volume of hepatocytes as a complementary method was estimated in addition to number estimation. Increased rabbit liver weight and volume were our primary observations, as the stereological assessment of the rabbit liver revealed a substantial rise in number as well as the volume of hepatocytes and sinusoidal spaces of the experimental group in comparison with the control groups. Our findings indicate that hyperplasia is the main reason for the increased total volume corresponding to the hepatocytes [31].

The main results of the two studies showed that MSCs, transplanted cells, have therapeutic effects on liver disease indirectly via secretion of soluble factors such as transforming growth factor β1 and prostaglandin E2. [35, 36]. In another study, administration of MSC lead to a reduction in liver fibrosis by producing soluble factors. Moreover, ADMSCs provid an immunomodulatory and an anti-inflammatory environment for stellate cells to preserve their phenotypes and avoid immune cell-mediated liver injury [37]. In agreement with our study, other groups showed that the histological changes improved, and inflammation and fibrosis diminished after MSC use [38]. In a study Amer et al. [39] included 40 patients

with end-stage liver failure, in which they divided them into two groups: one group was injected with pre-differentiated autologous bone marrow-derived MSCs; the other group was injected with standard supportive treatment. The results showed that the patients who received MSCs had improved in Child-Pugh and MELD scores following two weeks compared to the control groups [39, 40].

The current study illustrates the efficiency of stereology application in detecting triggered changes in liver tissue of rabbit fetuses after xenotransplantation of hWJ-MSCs. As a result, we report that the approach can be proficiently applied in studies that aim to detect and monitor possible changes in liver tissue after using a new treatment. Similarly, stereological factors offer helpful and reliable information for follow-up assessments in patients with chronic hepatitis B [41]. Stereology is a simple and reliable method for fulfilling quantitative measurement of liver elements, including the number and total volume of hepatocytes and sinusoids as well as central veins located in various areas of the liver post-xenotransplantation of hWJ-MSCs in rabbit fetus.

For the first time in this study, an increase in liver morphometric indices after human MSC xenotransplantation has been shown in rabbits. After xenotransplantation of human MSCs', rabbit liver tissue microenvironments altered quantitative factors of hepatocytes such as volume and density as well as their morphometric indices. Regardless of the success of differentiating human MSCs into hepatocytes, the effect of cell xenotransplantation on the morphometry of the liver may indicate concern in the function of xenotransplantation-produced human tissues. Considering the limitations of our findings, further research need to be conducted.

CONFLICTS OF INTEREST: None declared.

FINANCIAL SUPPORT: This work was supported by Vice-Chancellor of Research and Technology, Shiraz University of Medical Sciences (Grant no. 11489).

REFERENCES

1. Ebrahimi H, Naderian M, Sohrabpour AA. New Concepts on Pathogenesis and Diagnosis of Liver Fibrosis; A Review Article. *Middle East J Dig Dis* 2016;**8**:166-78.
2. Ekser B, Gridelli B, Tector AJ, Cooper DKJT. Pig liver xenotransplantation as a bridge to allotransplantation: which patients might benefit? *Transplantation* 2019;**88**:1041-9.
3. Lin S-Z, Chang Y-J, Liu J-W, *et al*. Transplantation of human Wharton's Jelly-derived stem cells alleviates chemically induced liver fibrosis in rats. *Cell Transplant* 2010;**19**:1451-63.
4. Ekser B, Markmann JF, Tector AJ. Current status of pig liver xenotransplantation. *Int J Surg* 2015;**23**:240-6.
5. Liu H, Kim Y, Sharkis S, *et al*. In vivo liver regeneration potential of human induced pluripotent stem cells from diverse origins. *Sci Transl Med* 2011;**3**:82ra39.
6. Naeem EM, Sajad D, Talaei-Khozani T, *et al*. Decellularized liver transplant could be recellularized in rat partial hepatectomy model. *J Biomed Mater Res A* 2019;**107**:2576-88.
7. Liu S, Jia Y, Yuan M, *et al*. Repair of osteochondral defects using human umbilical cord Wharton's jelly-derived mesenchymal stem cells in a rabbit model. *Biomed Res Int* 2017;**2017**:8760383
8. Beeram E. Hormonal effect on male fertility and stem cell survival. *J Infertil Reprod Biol* 2019;**7**:4-7.
9. Bongso A, Fong C-Y. The therapeutic potential, challenges and future clinical directions of stem cells from the Wharton's jelly of the human umbilical cord. *Stem Cell Rev Rep* 2013;**9**:226-40.
10. Wang HS, Hung SC, Peng ST, *et al*. Mesenchymal stem cells in the Wharton's jelly of the human umbilical cord. *Stem Cells* 2004;**22**:1330-7.
11. Kim D-W, Staples M, Shinozuka K, *et al*. Wharton's jelly-derived mesenchymal stem cells: phenotypic characterization and optimizing their therapeutic potential for clinical applications. *Int J Mol Sci* 2013;**14**:11692-712.
12. Kalaszczynska I, Ferdyn K. Wharton's jelly derived mesenchymal stem cells: future of regenerative medicine? Recent findings and clinical significance. *Biomed Res Int* 2015;**2015**:430847
13. Lu T, Yang B, Wang R, Qin C. Xenotransplantation: current status in preclinical research. *Front Immunol* 2020;**10**:3060.
14. Zhang Z, Bédard E, Luo Y, *et al*. Animal models in xenotransplantation. *Expert Opin Investig Drugs* 2000;**9**:2051-68.
15. Rezaeian L, Hosseini SE, Dianatpour M, *et al*. Intrauterine xenotransplantation of human Wharton jelly-derived mesenchymal stem cells into the liver of rabbit fetuses: A preliminary study for in vivo expression of the human liver genes. *Iran J Basic*

Med Sci 2018;**21**:89-96.

16. Fernandes DP, Pimentel MM, SANTOS FA, *et al*. Hematological and biochemical profile of BALB/c nude and C57BL/6 SCID female mice after ovarian xenograft. *Anais da Academia Brasileira de Ciências* 2018;**90**:3941-8.
17. Shah JA, Patel MS, Louras N, *et al*. Amino acid and lipid profiles following pig-to-primate liver xenotransplantation. *Xenotransplantation* 2019;**26**:e12473.
18. Junatas KL, Tonar Z, Kubíková T, *et al*. Stereological analysis of size and density of hepatocytes in the porcine liver. *J Anat* 2017;**230**:575-88.
19. Anderson AJ, Haus DL, Hooshmand MJ, *et al*. Achieving stable human stem cell engraftment and survival in the CNS: is the future of regenerative medicine immunodeficient? *Regen Med* 2011;**6**:367-406.
20. Osmanski BF, Lecarpentier E, Montaldo G, *et al*. Discriminative imaging of maternal and fetal blood flow within the placenta using ultrafast ultrasound. *Sci Rep* 2015;**5**:13394.
21. Tsagias N, Koliakos I, Karagiannis V, *et al*. Isolation of mesenchymal stem cells using the total length of umbilical cord for transplantation purposes. *Transfus Med* 2011;**21**:253-61.
22. Lanning D, Zhu X, Zhai SK, Knight KL. Development of the antibody repertoire in rabbit: gut-associated lymphoid tissue, microbes, and selection. *Immunol Rev* 2000;**175**:214-28.
23. Rezaeian L, Hosseini SE, Dianatpour M, *et al*. Production of Human Liver by Intrauterine Xenotransplantation of Human Wharton's Jelly-Derived Mesenchymal Stem Cells to Animal Fetus: A Review. *J Med Dent Sci* 2018;**6**:134-9.
24. Lopez-Tello J, Arias-Alvarez M, Jimenez-Martinez MA, *et al*. Competition for materno-fetal resource partitioning in a rabbit model of undernourished pregnancy. *PLoS One* 2017;**12**:e0169194.
25. Schoeberlein A, Holzgreve W, Dudler L, *et al*. In utero transplantation of autologous and allogeneic fetal liver stem cells in ovine fetuses. *Am J Obstet Gynecol* 2004;**191**:1030-6.
26. Young AJ, Holzgreve W, Dudler L, *et al*. Engraftment of human cord blood-derived stem cells in preimmune ovine fetuses after ultrasound-guided in utero transplantation. *Am J Obstet Gynecol* 2003;**189**:698-701.
27. Scherle W. A simple method for volumetry of organs in quantitative stereology. *Mikroskopie* 1970;**26**:57-60.
28. Nyengaard JR. Stereologic methods and their application in kidney research. *J Am Soc Nephrol* 1999;**10**:1100-23.
29. Mandarim-de-Lacerda CA. Stereological tools in biomedical research. *Anais da Academia brasileira de Ciências* 2003;**75**:469-86.
30. Khodabandeh Z, Dolati P, Zamiri MJ, *et al*. Protective Effect of Quercetin on Testis Structure and Apoptosis Against Lead Acetate Toxicity: an Stereological Study. *Biol Trace Elem Res* 2020;**199**:3371-81.
31. Karbalay-Doust S, Noorafshan A. Stereological study of the effects of nandrolone decanoate on the mouse liver. *Micron* 2009;**40**:471-5.
32. Altunkaynak BZ, Ozbek E. Overweight and structural alterations of the liver in female rats fed a high-fat diet: a stereological and histological study. T*urk J Gastroenterol* 2009;**20**:93-103.
33. Rohr H, Lüthy J, Gudat F, *et al*. Stereology of liver biopsies from healthy volunteers. *Virchows Arch A Pathol Anat Histol* 1976;**371**:251-63.
34. Martínez-Cerdeño V, Barrilleaux BL, McDonough A, *et al*. Behavior of xeno-transplanted undifferentiated human induced pluripotent stem cells is impacted by microenvironment without evidence of tumors. *Stem Cells Dev* 2017;**26**:1409-23.
35. Zhu X, He B, Zhou X, Ren J. Effects of transplanted bone-marrow-derived mesenchymal stem cells in animal models of acute hepatitis. *Cell Tissue Res* 2013;**351**:477-86.
36. Xagorari A, Siotou E, Yiangou M, *et al*. Protective effect of mesenchymal stem cell-conditioned medium on hepatic cell apoptosis after acute liver injury. *Int J Clin Exp Pathol* 2013;**6**:831-40.
37. Raicevic G, Najar M, Najimi M, *et al*. Influence of inflammation on the immunological profile of adult-derived human liver mesenchymal stromal cells and stellate cells. *Cytotherapy* 2015;**17**:174-85.
38. Harn H-J, Lin S-Z, Hung S-H, *et al*. Adipose-derived stem cells can abrogate chemical-induced liver fibrosis and facilitate recovery of liver function. *Cell Transplant* 2012;**21**:2753-64.
39. Amer M-EM, El-Sayed SZ, Abou El-Kheir W, e*t al*. Clinical and laboratory evaluation of patients with end-stage liver cell failure injected with bone marrow-derived hepatocyte-like cells. *Eur J Gastroenterol Hepatol* 2011;**23**:936-41.
40. de Miguel MP, Prieto I, Moratilla A, *et al*. Mesenchymal stem cells for liver regeneration in liver failure: from experimental models to clinical trials. *Stem Cells Int* 2019;**2019**:3945672.
41. Moudi B, Heidari Z, Mahmoudzadeh-Sagheb H. Study of liver in HBV-related hepatocellular carcinoma: Stereology shows quantitative differences in liver structure. *Eur J Histochem* 2018;**62**:2950.